

Research Advances

Zircon U-Pb Age of the Shangxu Gold Deposit from Bangong-Nujiang Co, Northern Tibet, and Restriction on the Early Cretaceous Orogenic Gold Mineralisation

HUANG Hanxiao^{1,*}, LI Guangming¹, LIU Hong¹, CAO Huawen¹ and ZHANG Zhilin²

¹ Chengdu Center, China Geological Survey, Chengdu 610081, China

² No.5 Geological Party of Tibet Geological Exploration Bureau, Golmud 816000, Qinghai, China

Objective

The Tibetan Plateau is the largest continent-to-continent collision belt in the world. Two orogenic gold mineralisation belts have been recognized in this collision belt, which are as follows: the Indus-Yarlung Zangbo suture zone orogenic gold belt (IYOG), represented by the Mayoumu and Bangbu gold deposits, and the Ailaoshan orogenic gold belt (AOG), whose typical cases include the Zhenyuan and Chang'an gold deposits. The IYOG formed during 54–45 Ma corresponds to the compressional deformation during the early stages of the collision of the plates of India and Eurasia, whereas the AOG formed in 38–29 Ma corresponds to that during the later stage of the collision. Recently, several medium- to large-sized gold deposits (e.g., the Dacha and Shangxu deposits) have been discovered along the Bangong Co-Nujiang suture belt, which indicates that another orogenic gold mineralisation belt existed within the Tibetan Plateau. However, the lack of a mineral suitable for dating or for altering the minerals that were affected by various tectonic thermal events causes difficulty to perform accurate dating. This study is based on the Shangxu gold deposit and analyses the genesis of zircon in gold-bearing quartz veins as well as the accurate gold-forming age by hydrothermal zircon micro probe analysis using the U-Pb (LA-ICP-MS) method.

Methods

Sample SX01, collected from the Shangxu quartz vein-type ore body of I-1, is 240 meters long and 2 meters wide with an average grade of 9.21 g/t. The wall rock consists of Middle to Lower Jurassic Mugangri Group metamorphic sandstone (Fig. 1a). The ore minerals include native gold, pyrite, galena and so on, which make up less than 5% of the content (Fig. 1b), and the non-

metallic minerals include quartz and calcite. The native gold is granular and finely scaled.

The zircon grains were selected from the gold-bearing quartz vein samples using the standard heavy mineral separation technology. Subsequently, the zircon granules that exhibited good transparency were selected using binoculars. The selected zircons were transformed into epoxy resin sample targets using the standard zircon 91500 (age 1062.4 Ma), which was then polished to the zircon center. After cleaning, the transmission light, reflected light and cathodoluminescence images were used to check the internal structure of zircon to perform dating. The U-Pb zircon dating and trace element testing (using LA-ICP-MS) of the sample was performed using the Agilent 7500a ICPMS with a Geolas2005 laser ablation system at the Key Laboratory of Geological Processes and Mineralogy Resources (GPMR), China University of Geosciences (CUG). The laser ablation was set to a spot size of 32 μm . Helium was used to carry the ablated material to the Agilent 7500a ICP-MS. The standard zircon Harvard 91500 and NIST610 were used to rectify the zircon partition and trace elements, respectively. The experimental data (Appendix 1) were processed by ICPMSDataCal, and the concordia plots and weighted mean U-Pb ages with 1σ were processed using the Isoplot 4.15 program.

Results

The zircons separated from the gold-bearing quartz veins were dark brown to black in colour. The grains ranged from 80 to 200 μm with several depicting short columnar and equigranular shapes with a few depicting hypidiomorphic and xenomorphic granules. The zircons in the auriferous quartz vein can be divided into hydrothermal zircons and inherited zircons captured from the wall rocks, and the inherited zircons can be further classified into magmatic zircons and detrital zircons from the Mugangri Group. The hydrothermal zircons are

* Corresponding author. E-mail: huanghanxiao1111@163.com.

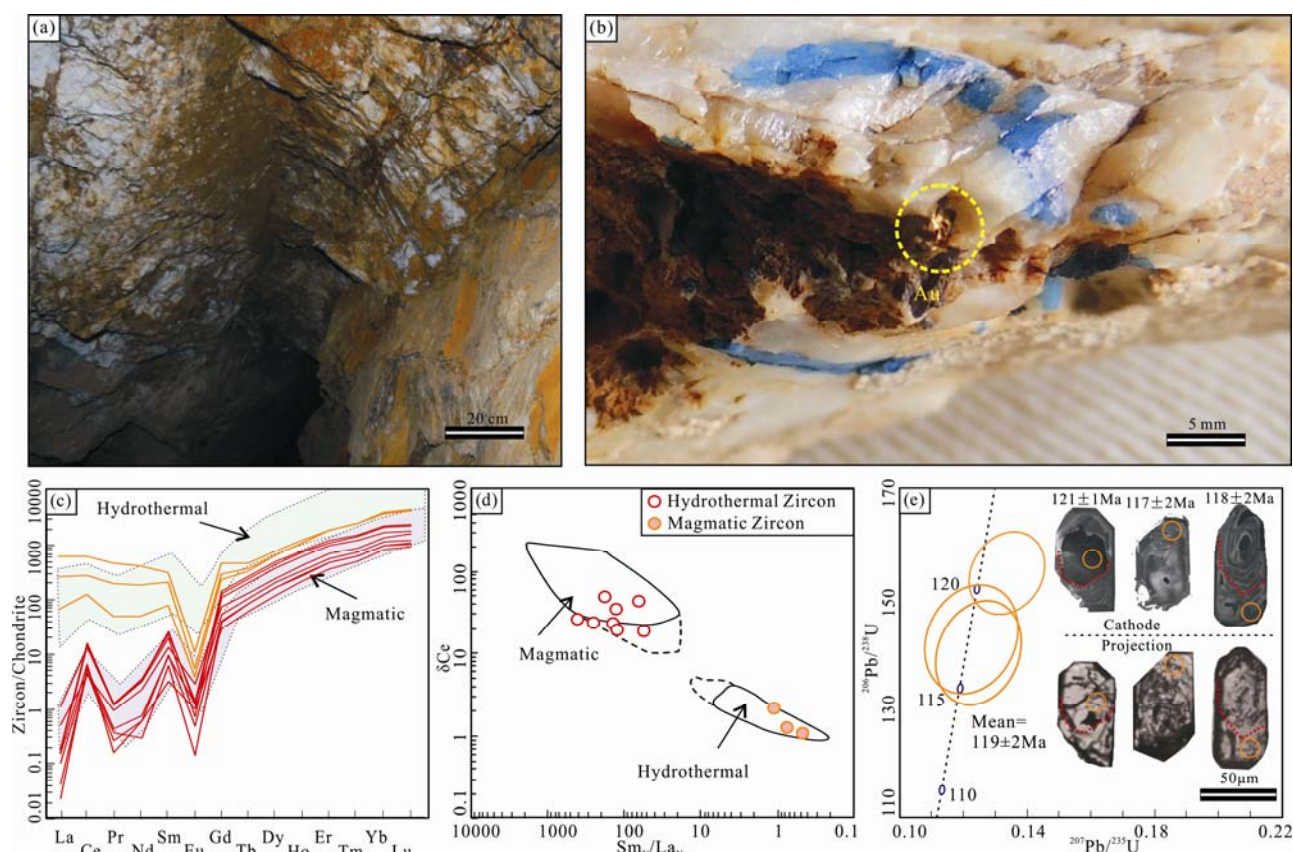


Fig. 1. Field photos and diagram of zircon and sericite in the Shangxu gold deposit.

characterized by absence of zoning and metasomatic texture, high total REE content, weak Ce positive and strong Eu negative anomalies on the chondrite-normalised REE patterns (Fig. 1c). These hydrothermal zircons fall in the hydrothermal zircon field in the $\delta\text{Ce}-\text{Sm}_N/\text{La}_N$ plots, (Fig. 1d) with low formation temperatures (approximately 470°C), and contain some inclusions. The hydrothermal zircons yield weighted mean ages of 119±2 Ma (Fig. 1e), which indicate that the Shangxu Au deposit has been subjected to a strong hydrothermal process during the Early Cretaceous period.

The Shangxu gold deposit was formed in the Muganggri Group, and it should be after the stratigraphic sedimentary, i.e., gold mineralisation occurred after the Middle Jurassic. The sericite in ore-bearing altered rocks is closely related to gold mineralisation. The results of the sericite $^{40}\text{Ar}-^{39}\text{Ar}$ isotope dating (Fig. 1g) exhibit that sericite was initially formed during the Late Jurassic Muganggri and that it was disturbed by the tectonic thermal events in the mid-Early Cretaceous; further, no related thermal events were observed to occur. Therefore, we suggest that the formation of the Shangxu gold deposit is most likely to be related to the hydrothermal events of the Early Cretaceous, i.e., the Shangxu gold deposit was

formed in the middle of the Early Cretaceous period.

Conclusions

The hydrothermal zircon dating results yielded a U-Pb age of 119±2 Ma, which corresponds not only to the early collision-extrusion deformation period between the Lhasa and Qiangtang terranes, but also to the placement of the intermediate-acid magma located in Muganggri Mountain (123±1 Ma). Based on the regional geological background, this study considered that there is a genetic relation between the Shangxu Au deposit and the acidic magma activities in the middle of the Early Cretaceous.

Acknowledgements

The manuscript benefited significantly from detailed reviews and constructive comments by Editors and reviewers. This study was financially supported by the National Key Research and Development Program of China (2016YFC0600308), the China Geological Survey Project (DD20160015, DD20160026), and the National Science Foundation (41702080, 41702086).

Appendix 1 LA-ICP-MS Zircon U-Pb Ages

Spot	Type	Ratio								Age (Ma)						Concordance	
		$^{207}\text{Pb}/^{206}\text{Pb}$	1 σ	$^{207}\text{Pb}/^{235}\text{U}$	1 σ	$^{206}\text{Pb}/^{238}\text{U}$	1 σ	$^{208}\text{Pb}/^{232}\text{Th}$	1 σ	$^{207}\text{Pb}/^{206}\text{Pb}$	1 σ	$^{207}\text{Pb}/^{235}\text{U}$	1 σ	$^{206}\text{Pb}/^{238}\text{U}$	1 σ	%	
1	Magmatic	0.0497	0.0027	0.1266	0.0066	0.0187	0.0002	0.0063	0.0003	183	128	121	6	120	2	99	
2	Hydrothermal	0.0481	0.0034	0.1202	0.0081	0.0182	0.0002	0.0057	0.0002	106	159	115	7	117	2	99	
3	Detrital	0.1588	0.0038	9.8194	0.2426	0.4444	0.0041	0.1243	0.0032	2444	41	2418	23	2370	18	97	
4	Hydrothermal	0.0482	0.0029	0.1255	0.0072	0.0189	0.0003	0.0060	0.0002	109	146	120	6	121	2	99	
5	Detrital	0.1069	0.0022	4.6726	0.1033	0.3153	0.0036	0.0914	0.0063	1747	38	1762	19	1767	18	99	
6	Detrital	0.1093	0.0022	4.6406	0.1000	0.3059	0.0036	0.1123	0.0069	1787	41	1757	18	1720	18	96	
7	Magmatic	0.0517	0.0040	0.1338	0.0104	0.0186	0.0002	0.0065	0.0003	333	180	128	9	119	2	93	
8	Detrital	0.1587	0.0040	9.7191	0.2605	0.4408	0.0053	0.1148	0.0031	2442	43	2409	25	2354	24	96	
9	Magmatic	0.0540	0.0020	0.1398	0.0050	0.0187	0.0002	0.0065	0.0002	372	83	133	4	120	1	90	
10	Magmatic	0.0498	0.0034	0.1257	0.0084	0.0188	0.0003	0.0067	0.0003	183	164	120	8	120	2	99	
11	Magmatic	0.0536	0.0022	0.1405	0.0056	0.0190	0.0002	0.0066	0.0002	354	91	133	5	121	1	90	
12	Detrital	0.1065	0.0023	4.4095	0.0966	0.2970	0.0026	0.1311	0.0063	1740	44	1714	18	1676	13	96	
13	Magmatic	0.0512	0.0018	0.1791	0.0065	0.0255	0.0003	0.0085	0.0003	250	81	167	6	162	2	97	
14	Hydrothermal	0.0528	0.0022	0.1399	0.0066	0.0189	0.0002	0.0062	0.0003	320	90	133	6	121	1	91	
15	Magmatic	0.0520	0.0029	0.1326	0.0071	0.0188	0.0003	0.0058	0.0002	287	121	126	6	120	2	95	
16	Magmatic	0.0499	0.0028	0.1272	0.0066	0.0187	0.0002	0.0059	0.0002	191	134	122	6	119	1	98	
17	Detrital	0.1050	0.0021	4.1872	0.0900	0.2857	0.0026	0.1226	0.0050	1713	37	1672	18	1620	13	95	
18	Magmatic	0.0503	0.0044	0.1310	0.0109	0.0189	0.0003	0.0055	0.0003	209	257	125	10	121	2	96	
19	Magmatic	0.0483	0.0076	0.1564	0.0249	0.0242	0.0007	0.0075	0.0005	122	328	148	22	154	3	96	
20	Hydrothermal	0.0483	0.0041	0.1202	0.0094	0.0182	0.0002	0.0059	0.0002	122	180	115	9	116	2	98	